ELSEVIER

Deep-Sea Research II 53 (2006) 250–269

DEEP-SEA RESEARCH
PART II

www.elsevier.com/locate/dsr2

Oceanographic characteristics of biological hot spots in the North Pacific: A remote sensing perspective

Daniel M. Palacios[a,b,*], Steven J. Bograd[b], David G. Foley[a,b], Franklin B. Schwing[b]

[a]*Joint Institute for Marine and Atmospheric Research, University of Hawaii, 1000 Pope Road, Marine Sciences Building, Room 312, Honolulu, HI 96822, USA*

[b]*NOAA/NMFS/SWFSC/Environmental Research Division, 1352 Lighthouse Avenue, Pacific Grove, CA 93950-2097, USA*

Received 20 May 2005; accepted 5 February 2006
Available online 27 April 2006

Abstract

Biological hot spots in the ocean are likely created by physical processes and have distinct oceanographic signatures. Marine predators, including large pelagic fish, marine mammals, seabirds, and fishing vessels, recognize that prey organisms congregate at ocean fronts, eddies, and other physical features. Here we use remote sensing observations from multiple satellite platforms to characterize physical oceanographic processes in four regions of the North Pacific Ocean that are recognized as biological hot spots. We use data from the central North Pacific, the northeastern tropical Pacific, the California Current System, and the Galápagos Islands to identify and quantify dynamic features in terms of spatial scale, degree of persistence or recurrence, forcing mechanism, and biological impact. The dominant timescales of these processes vary from interannual (Rossby wave interactions in the central North Pacific) to annual (spring-summer intensification of alongshore winds in the California Current System; winter wind outflow events through mountain gaps into the northeastern tropical Pacific), to intraseasonal (high-frequency equatorial waves at the Galápagos). Satellite oceanographic monitoring, combined with data from large-scale electronic tagging experiments, can be used to conduct a census of biological hot spots, to understand behavioral changes and species interactions within hot spots, and to differentiate the preferred pelagic habitats of different species. The identification and monitoring of biological hot spots could constitute an effective approach to marine conservation and resource management.

Keywords: Biological hot spots; Remote sensing; Upwelling; Eddies; Equatorial waves; Pacific Ocean

1. Introduction

Oceans are naturally heterogeneous on a wide range of spatial scales. The complexity of this environment creates a variety of habitats that marine organisms exploit throughout their life histories. Species have evolved to recognize and utilize particular features of their environment for locating food, avoiding predation, finding a mate, and producing young. Marine populations also tend to aggregate for reproduction, feeding, protection, and migration. Their ability to perform these functions is dependent not only on cues from other organisms, but on features of their physical environment. Locations where organisms tend to

*Corresponding author. NOAA/NMFS/SWFSC/Environmental Research Division, 1352 Lighthouse Avenue, Pacific Grove, CA 93940-2097,USA. Fax: +1 831 648 8440.
E-mail address: Daniel.Palacios@noaa.gov (D.M. Palacios).

0967-0645/$ - see front matter © 2006 Elsevier Ltd. All rights reserved.
doi:10.1016/j.dsr2.2006.03.004

concentrate regularly, or where there is high biological activity, are termed "biological hot spots". Because these areas feature high concentrations of organisms, including many species that are commercially exploited, they are often targeted for resource harvesting. Thus, biological hot spots must be an important facet of resource management and conservation efforts, including determining how to implement marine protected areas (MPAs), refugia, and fishery closures (Worm et al., 2003; Block et al., 2005).

A critical requirement in ecosystem-based resource management is learning how to define and identify biological hot spots, and characterizing them within the overall ocean environment. One aspect of this is to determine which physical attributes define a hot spot from an organism's point of view. This can be done through electronic tagging studies, which provide information on species aggregations and interactions in the context of the environment they are sampling (Block et al., 2002, 2005). A parallel effort is to assess the characteristics (e.g., size, life span, seasonality, persistence) of observable ocean features that could affect biological productivity and animal distributions. The combined use of these approaches allows for a more complete description of biological hot spots and a better understanding of pelagic habitat utilization by a variety of species.

Until recently, our understanding of the relationship between physical ocean structure and the distribution and behavior of top predators was limited to anecdotal reports, opportunistic sampling, simple correlations, and studies of limited temporal or spatial scope. Remote sensing has now become a powerful tool for monitoring ocean conditions on a global scale and at high spatial and temporal resolution. In addition, satellite data are increasingly being used to derive relevant ecosystem indicators (e.g., Polovina and Howell, 2005). In this paper, we use remote sensing observations from multiple satellite platforms to describe the oceanographic characteristics of four distinct environments in the North Pacific that encompass recognized biological hot spots, in terms of spatial scale, degree of persistence, recurrence, forcing mechanism, and biological impact. We also present a number of analytical approaches to characterize dynamic physical features that may lead to formation of biological hot spots in these different environments. This study provides a framework for a more complete characterization of biological hot spots that includes the oceanographic perspective.

2. Data sources and methods

2.1. Bathymetry

Digital bathymetry was extracted from the global sea floor topography of Smith and Sandwell (1997), version 8.2 (November 2000). This data set combines all available depth soundings with high-resolution marine gravity information provided by the Geosat, ERS-1/2, and TOPEX/Poseidon (T/P) satellite altimeters. It is available on line from the Institute of Geophysics and Planetary Physics at the Scripps Institution of Oceanography (http://topex.ucsd.edu/). The data set has a nominal resolution of 2 arc minutes (~4 km). A recent assessment of this data set relative to high-resolution (30 and 100 m) echosounder-derived multibeam surveys in the northeast Pacific found that the product performs well at identifying features to the scale of seamounts, but that subgrid-scale features in the satellite-derived bathymetry may vary from their true depth by up to 50% (Etnoyer, 2005).

2.2. Sea-level anomalies

Global, 7-day maps of gridded sea-level anomalies (SLA; i.e., the difference between the observed sea-surface height and the mean sea level, in cm) at 1/3-degree resolution on a Mercator projection (i.e., ~37 km at the equator and ~18.5 km at 60°N/S) were obtained for the period 14 October 1992–18 August 2004. SLA are relative to a 7-year mean (January 1993–January 1999). These maps are produced by combining data from the T/P, ERS-1/2, Jason, and Envisat satellite altimeters using the method described in Ducet et al. (2000). The data are produced by the Centre National d'études Spatiales (CNES, France) in partnership with its subsidiary Collecte, Localisation, Satellites (CLS) and local industry, for the Segment Sol multimissions d'ALTimétrie, d'Orbitographie et de localisation precise multimission ground segment (Ssalto) program, as part of the Data Unification and Altimeter Combination System (Duacs). The data are distributed by the Archiving, Validation, and Interpretation of Satellite Oceanographic data (Aviso) project (http://www.aviso.oceanobs.com/). Despite sampling error issues due to differing ground tracks and orbit repeat periods among

several altimeter instruments, merged data from multiple missions have the advantage of resolving oceanic mesoscale processes, which is beyond the capabilities of a single instrument (Fu et al., 2003).

2.3. Ocean color

Satellite-derived ocean color (phytoplankton chlorophyll-*a* concentration, or CHL, in $mg\,m^{-3}$) measured by the Sea-viewing Wide-Field-of-view Sensor (SeaWiFS) was obtained from a variety of sources for different purposes. For the general characterization in Section 3, we used monthly averages for the period September 1997–December 2004 at 9-km resolution. Selected monthly and 8-day averages were used for the case studies of the central North Pacific and the northeastern tropical Pacific in Sections 4.1 and 4.3, respectively. These 9-km data sets were obtained from the NASA Goddard Space Flight Center's (GSFC) Earth Sciences Data and Information Services Center Distributed Active Archive Center (GES DISC DAAC) (http://disc.gsfc.nasa.gov).

For the case study of the central California Current System in Section 4.2, daily SeaWiFS level-1a, Local-Area-Coverage (LAC) raw radiances were compiled from three sources for the period October 1997–March 2005. For October 1997–December 2004 data were provided by the Monterey Bay Aquarium Research Institute (MBARI) in collaboration with the University of California at Santa Cruz (UCSC) and NASA GSFC. For July 1998, data from MBARI's ground station were not available; data acquired by the University of California at Santa Barbara (UCSB) ground station and distributed by the GES DISC DAAC were used in their place. For January–March 2005 data were supplied by the NOAA National Ocean Service and NOAA CoastWatch under license to ORBIMAGE, Inc. The compiled raw radiances were processed to level-3 monthly mean CHL and projected onto a 0.0125×0.0125-degree resolution grid using NASA's SeaDAS software.

Finally, for the case study of the Galápagos Islands region in Section 4.4, daily level-2 Merged Local Area Coverage (MLAC) CHL data were obtained from NASA's Ocean Biology Processing Group (OBPG) distribution point (http://oceancolor.gsfc.nasa.gov/) for the period 4 October 1997–23 December 2004. Daily spatial subsets for the area bounded by 95–91°W, 2°S–1°N were processed to 8-day averages at a 0.0125-degree (1.39-km) resolution in SeaDAS.

2.4. Sea-surface temperature

Sea-surface temperatures (SST) derived from the Advanced Very High Resolution Radiometer (AVHRR) and processed with the NOAA/NASA AVHRR Oceans Pathfinder algorithm version 4.1 are distributed by the Physical Oceanography Distributed Active Archive Center (PO.DAAC) at the NASA/California Institute of Technology Jet Propulsion Laboratory (JPL) (http://poet.jpl.nasa.gov/). An 8-day average of best-quality, ascending-pass (daytime) data at 9 km resolution for the period 2–9 February 2003 is used in Section 4.3 to illustrate the case study of the northeastern tropical Pacific.

2.5. Analysis of monthly ocean color for central California

The combined data set of 0.0125-degree monthly CHL covering the period October 1997–March 2005 comprised 90 images. Empirical orthogonal function (EOF) analysis (Emery and Thomson, 1997; see also Kelly, 1988) of this data set was used to extract the characteristic patterns of CHL variability and identify potential biological hot spots off central California. Prior to analysis, a 5×5-pixel median smoother was applied to each image to remove small-scale noise. Few pixels were missing in most images due to persistent cloudiness, and these were interpolated with a single pass of a 5×5 median filter. The images for November 1997 and July 1998 had substantial gaps, and additional passes with 7×7 and 11×11 median filters were necessary to fill those gaps. After gap filling, each monthly image contained 151,249 valid pixels. Log-transformation of these data was necessary to homogenize the variance, an assumption of the EOF technique. To highlight potential biological hot spots (i.e. areas of enhanced CHL), the spatial mean was removed from each image (this approach is analogous to spatial detrending by removing the large-scale component in order to emphasize local variations above or below the spatial mean). The final step in the pre-treatment of the data set was the removal of the temporal mean at each pixel location. The results of the EOF analysis on these 151,249 spatial points (pixels) by 90 time steps (months) are presented in Section 4.2.

2.6. An index for the Galápagos plume

The physical and ecological factors leading to a plume of high phytoplankton biomass on the western side of the Galápagos Archipelago are described in Section 3.1.4. In order to quantify the scales of variability in this dynamic region, we used the 8-day CHL averages at 0.0125-degree (1.39-km) resolution for the area bounded by 95–91°W, 2°S–1°N. This data set comprised 329 images covering the period 4 October 1997–23 December 2004. Small-scale noise in each image was removed with a 3×3 median filter. The number of pixels in each image containing CHL $\geqslant 0.5\,\mathrm{mg\,m^{-3}}$ (a contour level that efficiently delineates the plume) was obtained and a Galápagos Plume Index (GPI) was derived by computing the area covered by these pixels. The total CHL biomass contained in this area was also computed. The resulting GPI time series are presented and discussed in Section 4.4.

3. Oceanographic characteristics of biological hot spots in the North Pacific

Biological hot spots are most often regarded as regions where top predators aggregate (Worm et al., 2003, 2005), presumably because of enhanced trophic interactions and feeding opportunities. From dynamical considerations, physical oceanographic features such as eddies, meanders, and fronts provide the mechanisms that result in aggregation and enhanced primary production (Flierl and McGillicuddy, 2002; Olson, 2002). While we recognize that biological hot spots also may occur in ocean regions that do not have discernable physical characteristics because they are used as fixed migratory corridors or reproductive destinations, our focus here is on the oceanographic features that lead to biological hot spots.

Oceanographic features can vary in terms of their spatial scales, their degree of persistence or recurrence, their forcing mechanisms, and their biological impacts. These characteristics are examined in this section, using four representative regions that encompass recognized biological hot spots: the central North Pacific (CNP), the central California Current System (CCS), the northeastern tropical Pacific (NETP), and the Galápagos Islands (Fig. 1). Descriptions of the general setting and the typical variability of these regions are presented in the following sections. Case studies illustrating the particular dynamics and the temporal variability in each region are given in Section 4.

3.1. Regional setting

3.1.1. The central North Pacific

Although hot spot activity is often most intense at relatively small spatial scales (tens of meters to a few hundred kilometers), coherent physical features can

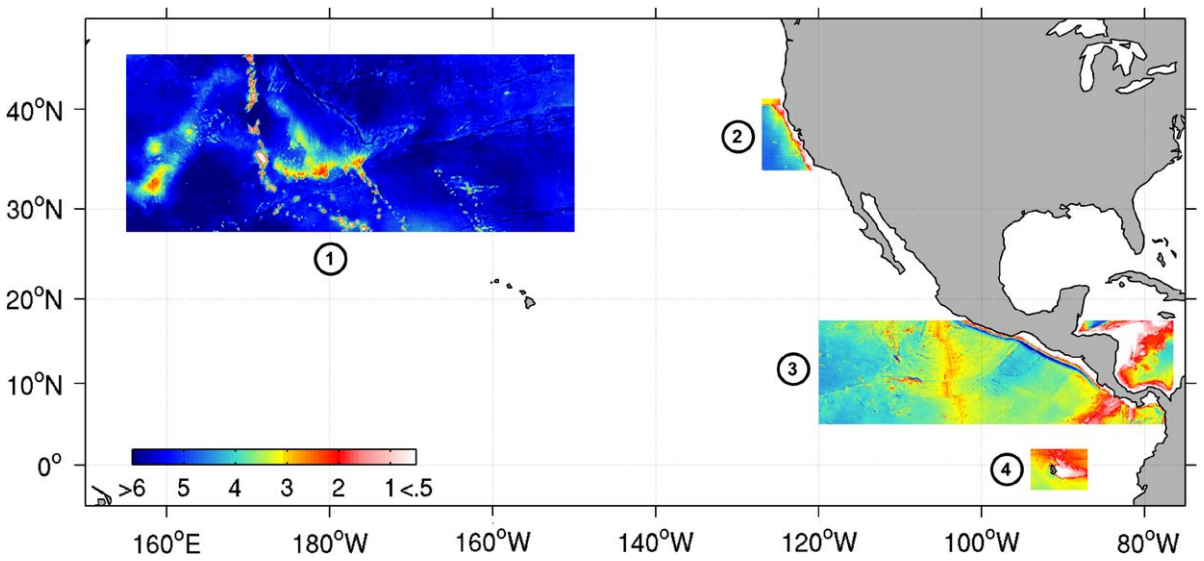

Fig. 1. Digital bathymetry v8.2 (in km) of Smith and Sandwell (1997) for four regions in the North Pacific. (1) Central North Pacific, (2) central California Current System, (3) northeastern tropical Pacific, and (4) Galápagos Islands.

extend across entire ocean basins. The region of the North Pacific bounded by 27.5–45°N, 155°E–150°W (Fig. 1) is representative of a number of processes that contribute to the development of large-scale, biologically utilized physical features. The CNP is far from coastal boundaries, is characterized by strong latitudinal gradients in light and nutrient availability (Glover et al., 1994; Chai et al., 2003), and is impacted by strong seasonality in large-scale wind forcing. A sharp transition from the high surface chlorophyll concentrations of the Subarctic Gyre to the low concentrations of the North Pacific Gyre is defined by the $0.2\,mg\,m^{-3}$ surface chlorophyll contour, and is known as the transition zone chlorophyll front (TZCF; Polovina et al., 2001). This frontal feature has been shown to be an important foraging and migratory habitat for a number of apex predators such as tuna, sea turtles, sharks, and seabirds (Laurs et al., 1984; Polovina et al., 2000, 2001, 2004), which leads to conflicts between migrating protected species and commercial fishing. Islands, seamounts, and sharp bathymetric gradients (Fig. 1) also contribute to the development of mesoscale physical features (Bograd et al., 1997; Seki et al., 2001). Blue whales (*Balaenoptera musculus*) occur year-round on the western part of the CNP (east of 170°E and north of 40°N), and tend to congregate around the Emperor Seamounts in winter months (Moore et al., 2002).

3.1.2. The central California Current System

Although a much smaller region than considered in the previous case, the region bounded by 34–40°N, 126°W to the coastal boundary (Fig. 1) is characterized by very strong cross-shore gradients in physical and biological fields, is strongly modulated by seasonal wind forcing and Ekman dynamics, has a complex and energetic current structure, and is greatly influenced by a heterogeneous continental shelf topography and coastal orography (Hickey, 1979). This is a highly productive eastern boundary current system, driven by seasonal coastal upwelling, which maintains numerous economically important marine fisheries. Heavy fishing effort in this region in combination with natural environmental variability has resulted in a number of overfished stocks (e.g., NMFS, 1999; Jacobson et al., 2005). This region is also home to a series of federal marine sanctuaries (Fig. 11A) and state reserves, and is being considered for the establishment of MPAs.

3.1.3. The northeastern tropical Pacific

Further south, the region of the eastern tropical Pacific bounded by 5–17.5°N, 120–76.5°W (Fig. 1) is dominated by complex offshore bathymetry and rugged coastal orography. The NETP is greatly impacted by wintertime wind jets passing through mountain gaps along the Central American isthmus (Chelton et al., 2000), which lead to the development of upwelling plumes (Clarke, 1988; Legeckis, 1988; Trasviña et al., 1995) and numerous westward-propagating eddies readily detectable in satellite SST and CHL imagery (Hansen and Maul, 1991; Müller-Karger and Fuentes-Yaco, 2000; Gonzalez-Silvera et al., 2004). Further offshore, seasonally intensified cyclonic wind stress curl associated with the intertropical convergence zone forces a broad thermocline ridge along 8°N between the westward-flowing North Equatorial Current and the eastward-flowing North Equatorial Countercurrent. At the eastern terminus of this shallow ridge is the Costa Rica Dome, another center of enhanced biological production in the NETP (Fiedler, 2002). The NETP is a diverse and highly productive tropical ecosystem, which supports an industrial tuna fishery and other top predators (Reilly and Thayer, 1990; Fiedler, 2002). This region is also the stage of the tuna-dolphin conservation issue (Gerber et al., 1999; Hall and Donovan, 2001).

3.1.4. The Galápagos Islands

On smaller scales, the region bounded by 2°S–2°N, 92.5–88°W (Fig. 1) contains the Galápagos Islands, which represent a steep topographic barrier within a deep oceanic environment approximately 960 km off the coast of South America. The physical and ecological factors leading to a plume of high phytoplankton biomass (CHL $\geqslant 0.5\,mg\,m^{-3}$) on the western side of the archipelago include the localized, year-round topographic upwelling of the Equatorial Undercurrent, seasonal wind-driven upwelling along the equatorial cold tongue, and natural iron enrichment from the island platform (Feldman, 1986; Coale, 1998; Palacios, 2002, 2004). On average, the plume covers an area of about $25{,}000\,km^2$ and has a westward extent of about 120 km (Palacios, 2002). Its biological effects are evident from the high densities of marine mammals within the plume (Palacios, 1999, 2003; Palacios and Salazar, 2002; Salazar, 2002). This region is subject to strong interannual variations (i.e. El Niño and La Niña events) that greatly impact the local marine

biota that depend on the upwelling (Boersma, 1978; Feldman et al., 1984; Robinson and del Pino, 1985; Valenti et al., 1999). This region is a textbook example of endemism, speciation, and biodiversity resulting from strong environmental pressures (James, 1991; Grant, 1999). The oceanic region surrounding the Galápagos is a National Marine Reserve (Fig. 5A), declared by the Government of Ecuador (Heylings et al., 2002), with a number of serious conservation issues (e.g., Boersma et al., 2005).

3.2. The mean state

Although many hot spots are patchy and ephemeral (e.g., open-ocean eddies or small-scale fronts), physical features that are relatively fixed spatially or that persist through time may be more ecologically relevant. Such persistence is conducive to food chain development and trophic interactions from primary producers up to the highly mobile nekton. Similarly, processes that repeat on regular cycles (e.g., seasonal coastal upwelling in eastern boundary current systems) can lead to the predictable development of exploitable foraging regions year after year. Many marine species have evolved to synchronize their life cycles to the presence (or absence) of these persistent and repeatable features (Cushing, 1990).

Seasonal mean maps of SLA and CHL are used to represent the background physical and biological environments of each region, respectively, and can be used to identify persistent and repeatable features (Figs. 2–5). Across the open CNP, SLA has large positive and negative amplitudes along a zonal band centered near 30–35°N, with the strongest positive anomalies occurring in summer (Fig. 2B) over the rugged submarine topography west of the dateline (Fig. 1). In winter, a persistent band of negative anomalies extends southwest from the northwestern boundary of the Subarctic Gyre (Fig. 2A). Associated with this band of negative anomalies is the southward extension of the TZCF (Fig. 2C). Relatively high (low) CHL covers most of the central North Pacific region in winter (summer), reflecting seasonal interactions between light and nutrient availability. The TZCF migrates seasonally over approximately 10 degrees of latitude, although there is significant interannual variability in its seasonal range and wintertime southerly extent (Bograd et al., 2004).

Compared to the CNP, the CCS has a much smaller seasonal range in SLA (Fig. 3A and B). The SLA gradients, however, can be high, and reflect important seasonal dynamics. The cross-shore SLA gradient in the CCS reflects the persistent equatorward flow of the California Current, while the larger offshore anomalies in summer reflect the seasonal development and offshore propagation of mesoscale eddies following the spring transition (Strub et al., 1987; Chereskin et al., 2000; Lynn et al., 2003). Long-lived mesoscale eddies in the CCS have been implicated in retention

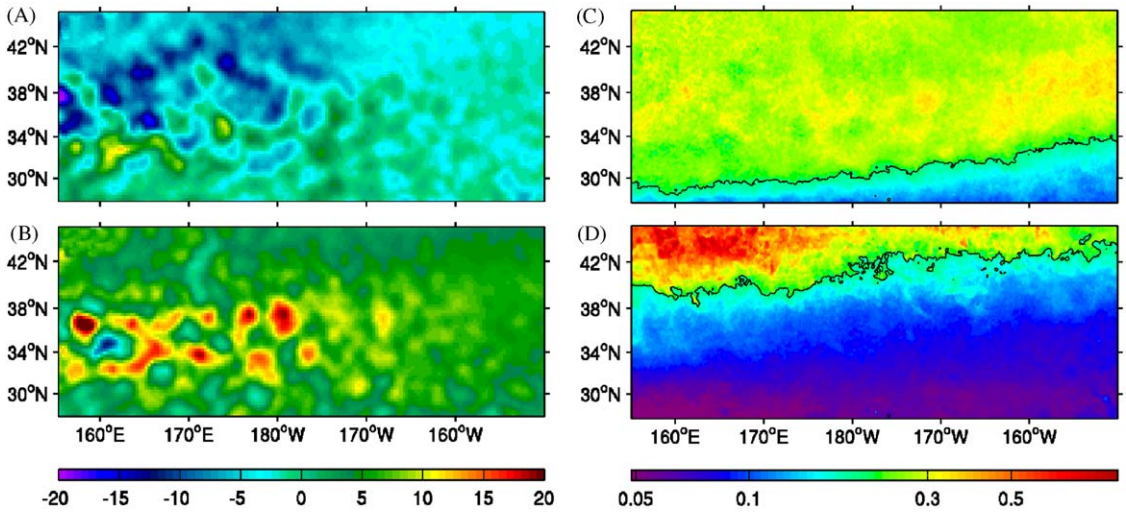

Fig. 2. Mean SLA (A, B; in cm) and mean CHL (C, D; in mg m^{-3}) for February and August for the central North Pacific. CHL fields in this figure and in Figs. 3–9 were smoothed with a 3×3-pixel median filter to remove small-scale noise. Black line in (C) and (D) is the 0.2 mg m^{-3} contour representing the TZCF.

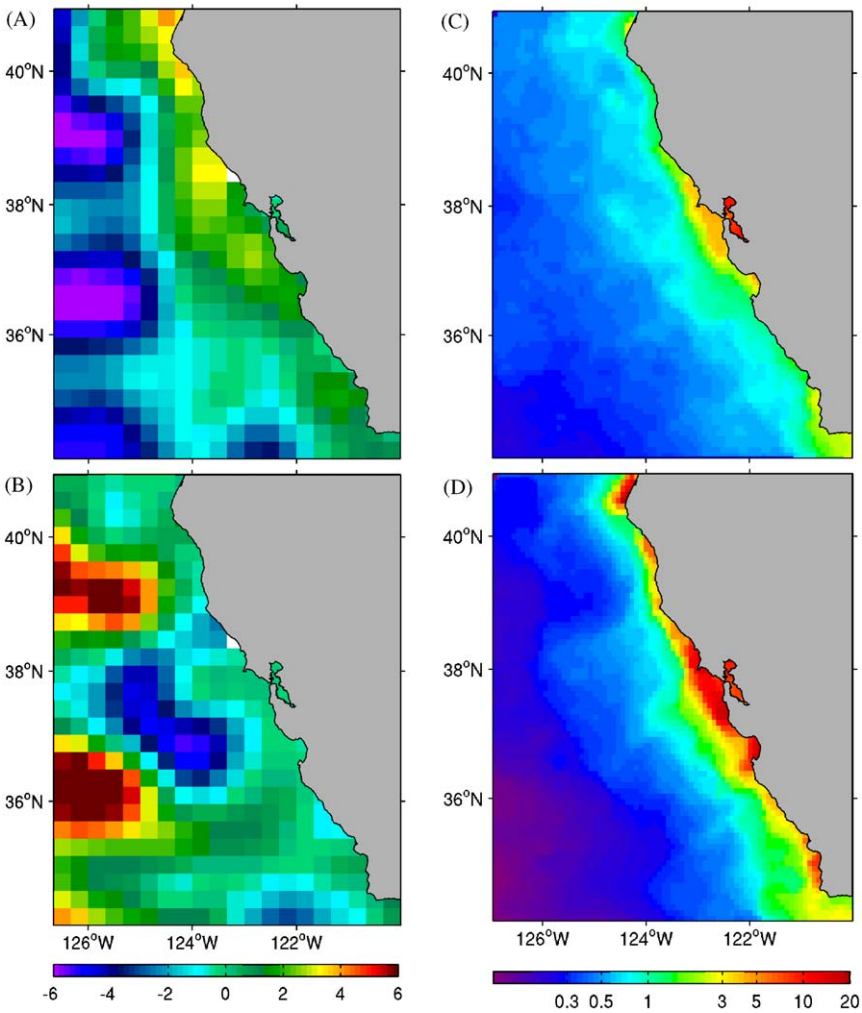

Fig. 3. Mean SLA (A, B; in cm) and mean CHL (C, D; in mg m^{-3}) for February and August for the central California Current System.

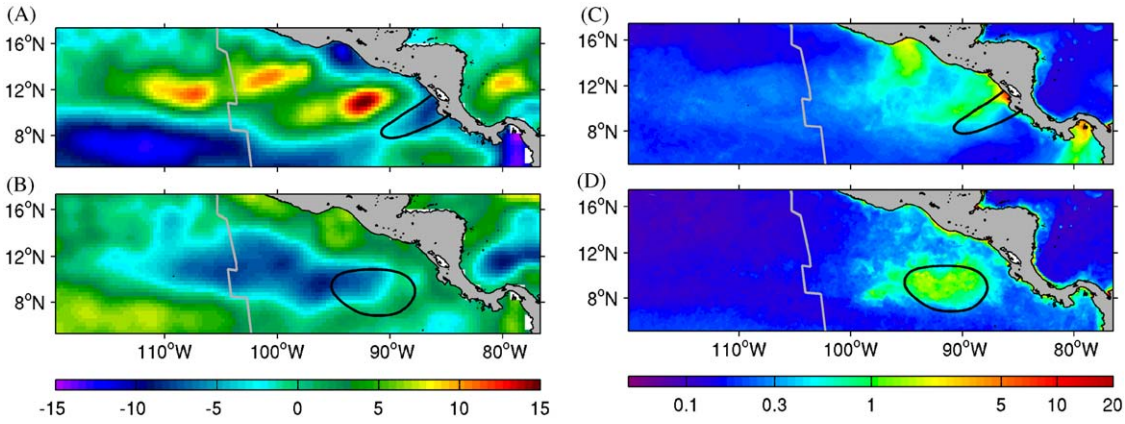

Fig. 4. Mean SLA (A, B; in cm) and mean CHL (C, D; in mg m^{-3}) for February and August for the northeastern tropical Pacific. Black contour in each panel is the corresponding mean location of the Costa Rica Dome, as outlined by the 20 °C isotherm depth at 35 m, courtesy of Paul C. Fiedler (NOAA/NMFS/SWFSC). Gray line marks the axis of the East Pacific Rise.

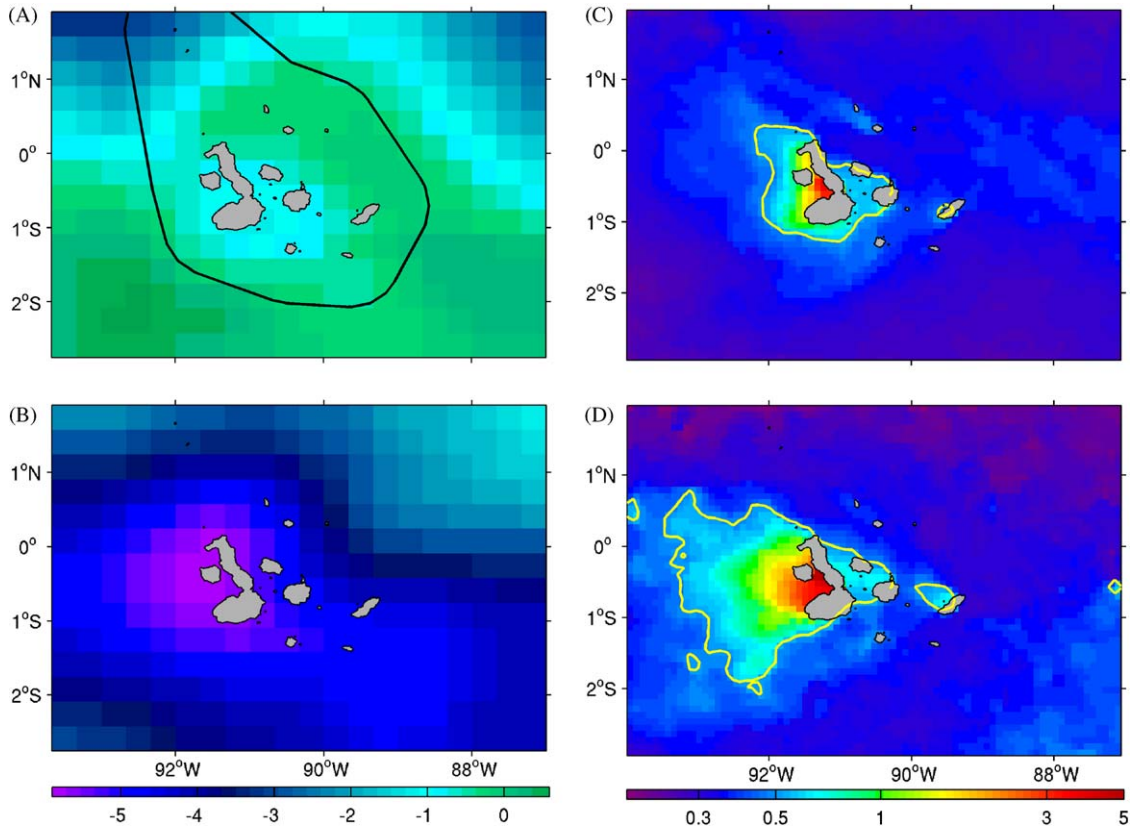

Fig. 5. Mean SLA (A, B; in cm) and mean CHL (C, D; in mg m^{-3}) for February and August for the Galápagos Islands. Black line in (A) is the boundary of the Galápagos Marine Reserve, courtesy of the Unidad de Zonificación, Servicio Parque Nacional Galápagos, Ecuador. Yellow line in (C) and (D) is the outline of the Galápagos Plume, as indexed by the 0.5 mg m^{-3} CHL level.

and recruitment of coastal pelagic fish species (Logerwell and Smith, 2001). Seasonal coastal upwelling in the CCS leads to very high summertime CHL at the coast, and strong cross-shore gradients (Fig. 3D).

There is a marked seasonal contrast in SLA in the NETP (Fig. 4A and B). In winter, a band of high anomalies extending westward from Central America at about 10–15°N reflects the persistent formation of eddies in the Gulfs of Tehuantepec and Papagayo and their offshore propagation (Fig. 4A; Palacios and Bograd, 2005). A break in the high SLA along the path of Tehuantepec eddies is apparently associated with the East Pacific Rise (Palacios and Bograd, 2005). In contrast to this pattern, summer in the eastern tropical Pacific is quiescent (Fig. 4B). At this time, zonal thermocline ridging, peaking at the Costa Rica Dome, results in relatively low mean SLA and elevated CHL (Fig. 4B and D). High wintertime CHL squirts extend offshore from the Gulfs of Tehuantepec, Papagayo, and Panamá, driven by local upwelling resulting from intense wind jets blowing through mountain gaps along Central America (Fig. 4C). This also results in negative SLAs at the Gulfs of Tehuantepec and Papagayo (Fig. 4A). The zonal band characterized by strong eddy activity in winter also corresponds with relatively higher CHL.

The region around the Galápagos has weak seasonality in SLA (Fig. 5A and B). SLAs are mostly negative, especially in August, when equatorial divergence and upwelling are strongest (Palacios, 2004). The Galápagos high-CHL plume resulting from the topographic upwelling of the Equatorial Undercurrent is present year-round, but becomes more evident in August due to the additional forcing of upwelling-favorable southeast trade winds at this time of the year (Fig. 5C and D).

3.3. Variations around the mean state

Strong and persistent perturbations from the mean background state in a region may be

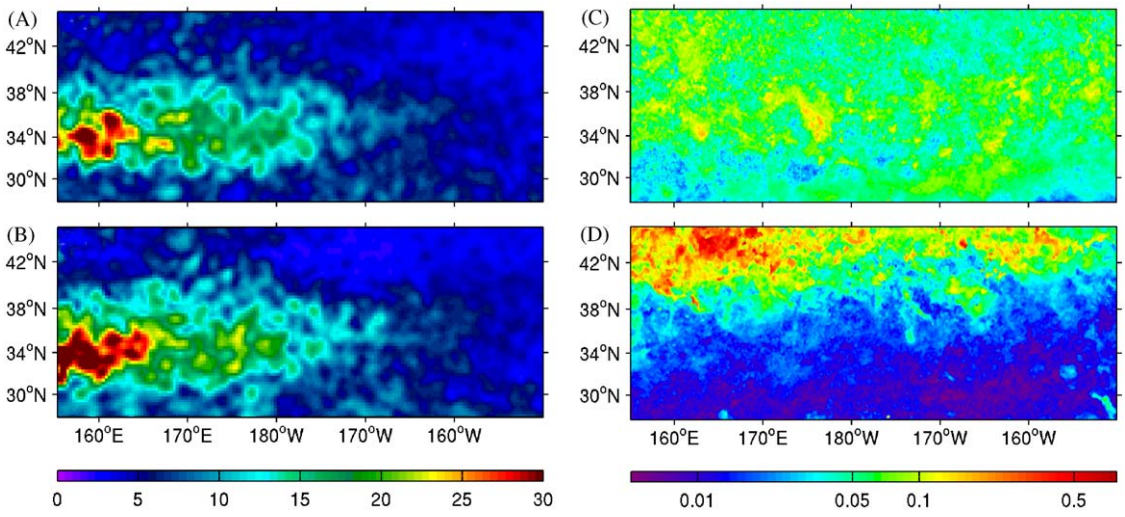

Fig. 6. RMS SLA (A, B; in cm) and RMS CHL (C, D; in mg m^{-3}) for February and August for the central North Pacific.

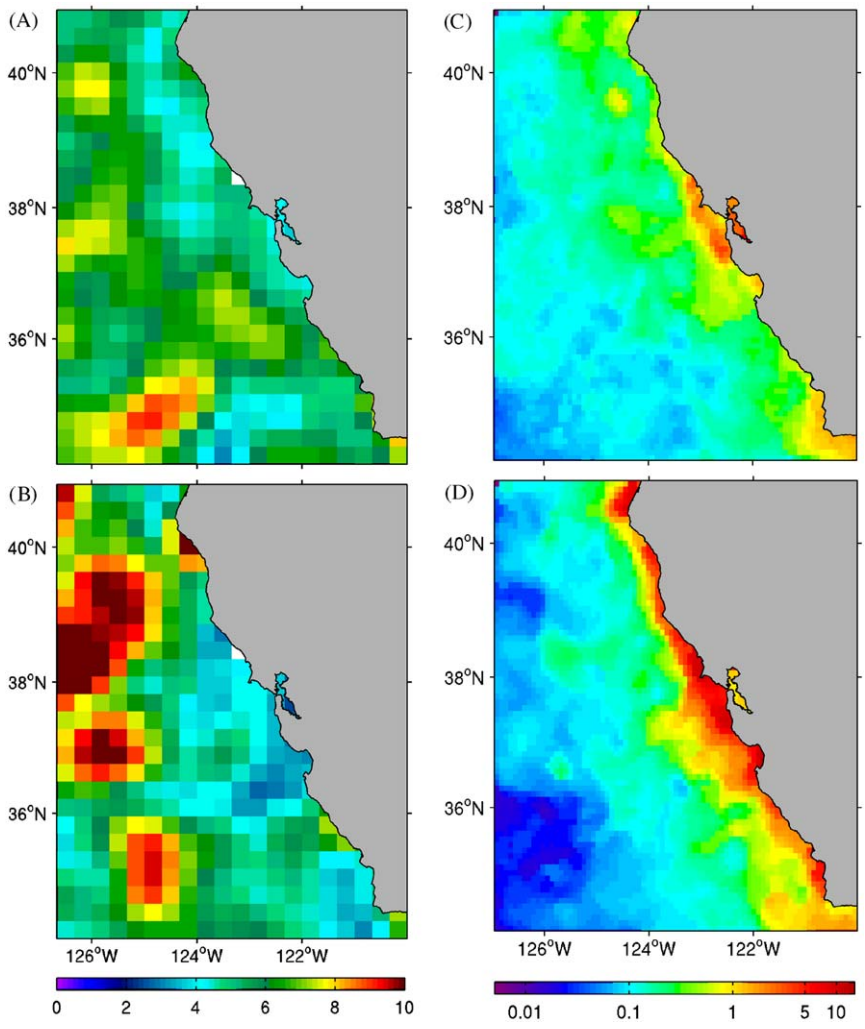

Fig. 7. RMS SLA (A, B; in cm) and RMS CHL (C, D; in mg m^{-3}) for February and August for the central California Current System.

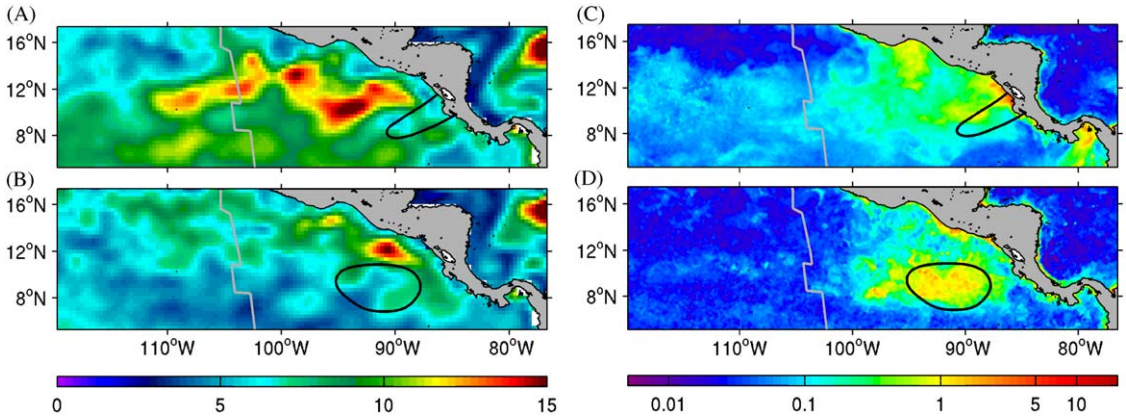

Fig. 8. RMS SLA (A, B; in cm) and RMS CHL (C, D; in mg m^{-3}) for February and August for the northeastern tropical Pacific. Black contour in each panel is the corresponding mean location of the Costa Rica Dome, as outlined by the 20°C isotherm depth at 35 m, courtesy of Paul C. Fiedler (NOAA/NMFS/SWFSC). Gray line marks the axis of the East Pacific Rise.

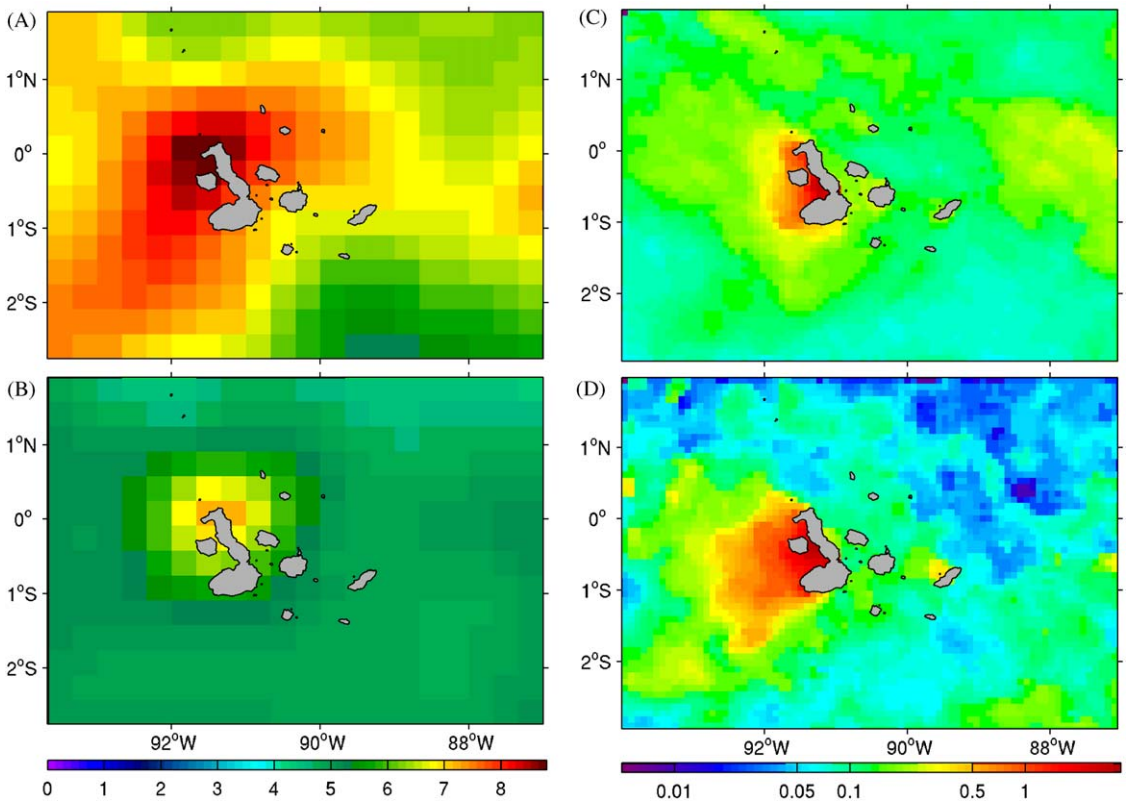

Fig. 9. RMS SLA (A, B; in cm) and RMS CHL (C, D; in mg m^{-3}) for February and August for the Galápagos Islands.

indicative of the formation of dynamic oceanographic features. Seasonal maps of root-mean-square (RMS) SLA and RMS CHL capture the magnitude, location, and persistence of enhanced physical-biological variability within each region (Figs 6–9). There is little seasonal variability in RMS SLA in the CNP, with highest energies consistently found in the region around 32–36°N west of the dateline (Fig. 6A and B). Much of the observed variability in this region is due to eddies shed from the Kuroshio Extension (e.g., Qiu, 1995). The eastern side is also replete with mesoscale

features consistent with the passage of long Rossby waves propagating westward from the North American coast (e.g., van Woert and Price, 1993; Fu and Qiu, 2002). The highest variability in the RMS CHL field is coincident with the high-energy eddy field in winter, but migrates northward with the TZCF in summer (Fig. 6C and D). The broad zones of high RMS CHL around 32–36°N in winter and 38–42°N in summer reflect interannual variability in the seasonal range of the TZCF.

The highest eddy energies in the CCS occur in the offshore region, and reflect the year-round presence of the meandering California Current, as well as offshore-propagating features associated with summertime coastal upwelling (Fig. 7A and B). Highest CHL variability in the CCS is confined year-round to the upwelling zone along the shelf, but is strongest in the peak upwelling months in spring and summer (Fig. 7C and D).

In the NETP, the winter months are characterized by a much more energetic eddy field than the summer months, as is evidenced by the mean SLA fields (Fig. 8A and B). Highest eddy energies are found within the region of eddy propagation away from the Central American coast. The CHL variability responds to these seasonally varying physical processes (Fig. 8C and D). Winter wind jets create upwelling plumes off the Gulfs of Tehuantepec, Papagayo, and Panamá, as well as highly variable CHL content in the westward propagating eddies. The Costa Rica Dome is most strongly developed in summer, and corresponds with the highest CHL RMS.

SLA variability is small at the Galápagos compared to the other regions (Fig. 9A and B). A more energetic SLA field is seen in February, especially where the Equatorial Undercurrent upwells. Variations within the CHL plume on the western side of the islands are evident throughout the year, but are strongest in August (Fig. 9C and D).

4. Case studies

4.1. The central North Pacific

The June 1999 mean SLA and CHL fields provide a case study of physical-biological coupling at oceanographic features spanning a wide range of spatial scales over the central North Pacific (Fig. 10). On the basin scale, the TZCF extends from 37°N, 150°W across the entire width of the region to 33°N, 155°E, with a well-defined wavelike pattern of ~300–500 km wavelength (Fig. 10B). This is a dynamic region separating low-nutrient, oligotrophic subtropical waters to the south from high-nutrient, high CHL waters to the north. The SLA field also shows a similar wavelike pattern spanning the same meridional range across the basin, with the height anomalies intensifying to the west (Fig. 10A).

At the mesoscale, there is a direct correspondence between the SLA eddy field and local CHL content. (Note that because a spatially sloping surface is removed from the absolute altimetry measurements of sea level, some of these features may be meanders rather than closed eddies.) The cyclonic (anticyclonic) features in Fig. 10 are clearly associated with locally high (low) CHL, reflecting the subsurface upwelling (downwelling) associated with surface divergence (convergence). This coupling can be seen in the intense eddy field near the western boundary of the region, as well as in the weaker line of eddies that span the basin near 28°N. Similar correspondences are found year-round in this region. This relationship demonstrates that the waters within and south of the TZCF are nutrient-limited, and require vertical motions to inject nutrients into the euphotic zone and induce primary production, as has been demonstrated in other oligotrophic gyral systems (e.g., McGillicuddy and Robinson, 1997; McGillicuddy et al., 1998).

Interannual variability in SLA along 36°N (Fig. 10C) reveals the persistence and westward propagation of the eddy field, with greatest energy west of the dateline. Alternating bands of relatively high and low SLA can be tracked for two years or more in Fig. 10C, with a westward propagation speed of ~3–5 km d^{-1}. This is consistent with the propagation of first-mode baroclinic Rossby waves, which have been shown to dominate the propagating component of altimetry-derived sea surface height fields (Chelton and Schlax, 1996; Stammer, 1997; Polito and Cornillon, 1997; Cipollini et al., 1997; Uz et al., 2001). The vertical isopycnal displacements associated with the negative SLA features will introduce nutrients into the euphotic zone, thus stimulating primary production (Uz et al., 2001; Cipollini et al., 2001; Sakamoto et al., 2004). Uz et al. (2001) and Sakamoto et al. (2004) found a strong coherence between satellite-derived propagating SLA and CHL signatures in the midlatitude oceans, with nutrient injection upon passage of Rossby waves being the dominant

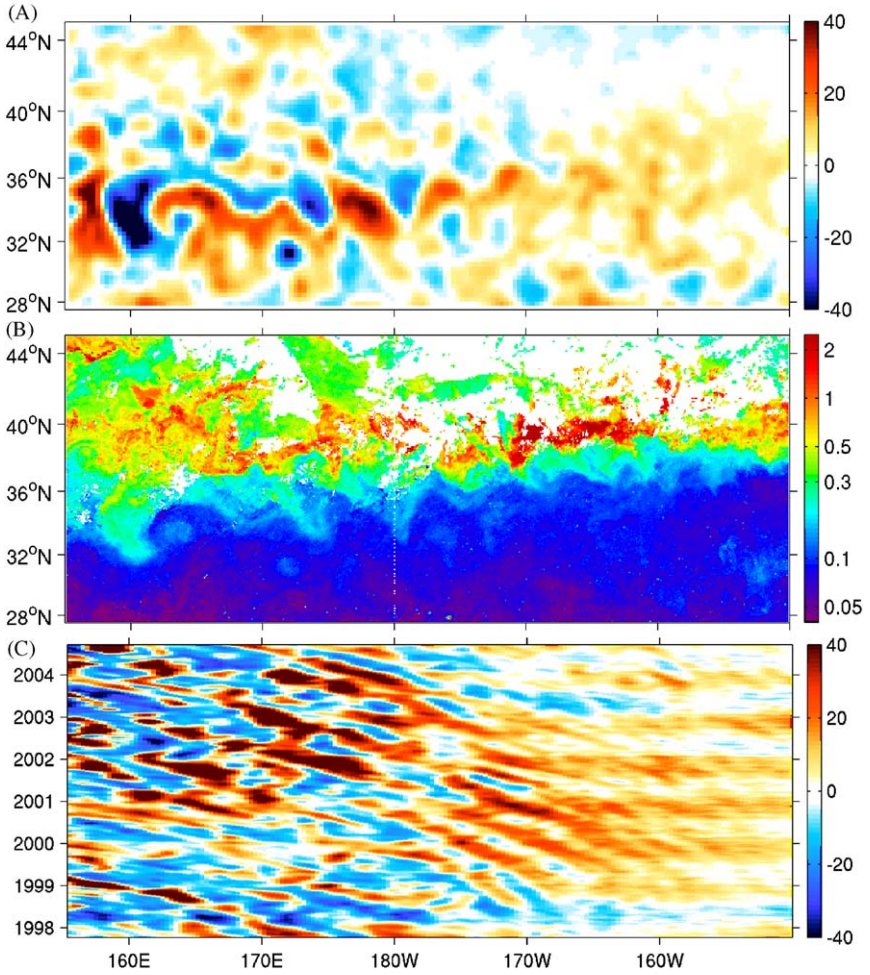

Fig. 10. Case study for the central North Pacific region. (A) SLA (in cm) for the 7-day period 3–9 June 1999, (B) monthly averaged CHL (in $mg\,m^{-3}$) for June 1999 (persistent cloudiness in this region often precludes the use of shorter-term averages), and (C) Hövmöller diagram of SLA along 36°N for the period September 1997 to August 2004. SLA range is restricted for display purposes; values as low as −63 cm (−47 cm) and as high as +49 cm (+86 cm) occur at the strongest features in panel A (panel C).

mechanism. The persistence of these propagating disturbances implies the continual presence of locally high patches of primary production, and may explain why a number of apex predators heavily utilize the front. It is also clear, however, that there is significant interannual variability in the frequency and magnitude of these disturbances (Fig. 10C).

4.2. The central California Current System

The first three modes of an EOF decomposition (see Section 2.5), explain 41.4% of the variance in the data set (Fig. 11). The dominant mode (26.2%) describes an onshore-offshore contrast (Fig. 11A), varying on a characteristic annual cycle: the minimum is reached around December–January and the maximum occurs as a broad peak in May–July (Fig. 11D). Three distinct zones of enhanced CHL are seen along the coast (Fig. 11A). From north to south these are: Cape Mendocino to Point Arena; Bodega Head to Point Sur; and Cape San Martin to Point Arguello. The latter extends south and offshore as a plume that includes the north side of the westernmost Channel Islands (San Miguel and Santa Rosa). Within this last zone, Estero (Morro) Bay and the Santa Maria Basin have the strongest enhancements. These three zones of persistently high CHL are associated with known upwelling centers along the coast

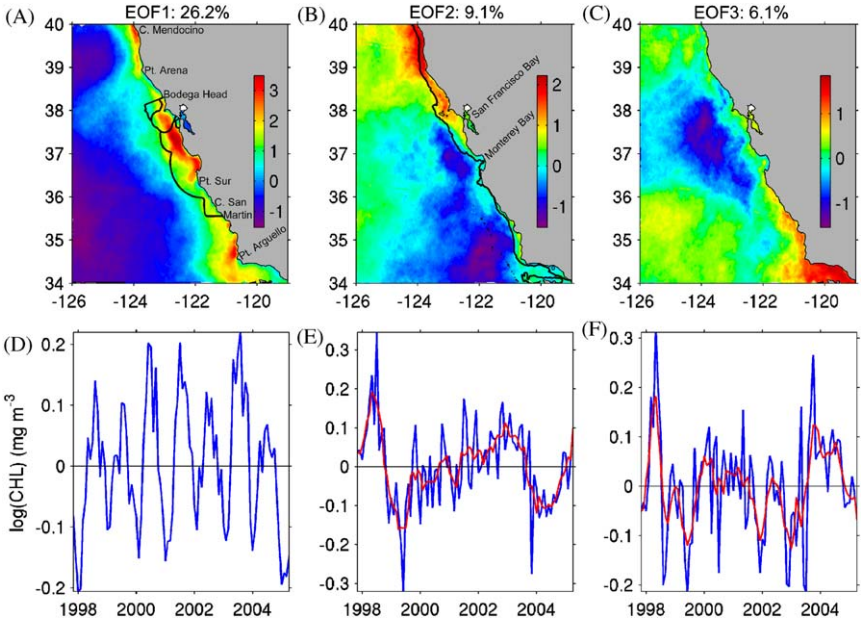

Fig. 11. Case study for the central California Current System region. The first three modes (A–C) of an EOF decomposition of monthly averaged, 1-km resolution CHL (after log-transformation; see Section 2.5 for details) for the period October 1997–March 2005. Panels in bottom row (D–F) show the corresponding amplitude time series (red series in the last two panels are the 5-point running averages). Black lines in panel A are the boundaries of the NOAA-designated Cordell Bank, Gulf of the Farallones, and Monterey Bay National Marine sanctuaries (from north to south), courtesy of Chad King (NOAA/NOS/MBNMS). Black contour in panel B is the 200-m isobath from the Smith and Sandwell (1997) bathymetry.

(Hickey, 1979; Dorman and Winant, 1995), and possibly represent areas of enhanced foraging opportunities for migratory species and top predators in the CCS.

The second (9.1% of the variance) and third (6.1%) modes are characterized by high-frequency variability (Fig. 11E and F) possibly representing short-lived events not fully resolved by the monthly composites. However, a clear interannual signal is also present in both modes (as illustrated by the 5-point running averages in Fig. 11E and F). Mode 2 describes a narrow band of CHL enhancement along the coast that widens northward of San Francisco Bay (Fig. 11B). The shape of this band closely follows the edge of the continental shelf, as outlined by the 200-m isobath, especially south of San Francisco Bay. Although not evident at the scale of the map, CHL patterns over local bathymetric features like the Monterey Canyon System are resolved by this mode. The interannual behavior of this mode (Fig. 11E) shows a strong, broad peak coinciding with the 1998–99 La Niña event, followed by a positive trend for the period May 1999–November 2002, at which time there is a rapid decrease associated with the 2002–2003 El Niño lasting until November 2003. Finally, there is a rapid increase until the end of the series (Fig. 11E). The positive trend over the period May 1999–November 2002 is consistent with a recent study for the 6-yr period 1998–2003 that reported global CHL increases of 10.4% for the coastal region, and of 60.3% specifically for the California/Mexican shelf (Gregg et al., 2005).

Mode 3 describes enhanced CHL levels in the Santa Barbara Channel and to a lesser extent at various locations along the coast, including inside San Francisco Bay (Fig. 11C). A region of reduced CHL sits offshore in the central part of the study area. The low-frequency temporal behavior of this mode (Fig. 11F) describes winter/springtime peaks in 1998, 2000, and 2004. The largest peak occurs in February–April 1998, at a time when severe winter storms over California following the 1997–1998 El Niño resulted in heavy coastal runoff and plumes containing elevated levels of suspended sediment (Mertes and Warrick, 2001), as well as CHL and colored dissolved organic matter extending offshore (Kudela and Chavez, 2004). Thus, it is possible that

mode 3 is capturing the effects of riverine input to the coastal zone, particularly during winter/springtime. Warmer water temperatures and the sheltered condition of the Santa Barbara Channel may account for the higher CHL in the southern part.

As mentioned above, the three zones of persistently high CHL identified in mode 1 (Fig. 11A) may be of special importance for marine predators in the CCS. Indeed, the importance of the central zone (Bodega Head to Point Sur) to resident as well as far-ranging marine birds and mammals is well known (e.g., Yen et al., 2004; Croll et al., 2005; Keiper et al., 2005). This zone is well covered by three adjacent NOAA National Marine Sanctuaries: Cordell Bank, Gulf of the Farallones, and Monterey Bay (Fig. 11A). The southern zone is only protected around the Channel Islands, although its importance for top predators has also been documented (e.g., Croll et al., 1998; Fiedler et al., 1998). No protected areas have been designated in the northern zone.

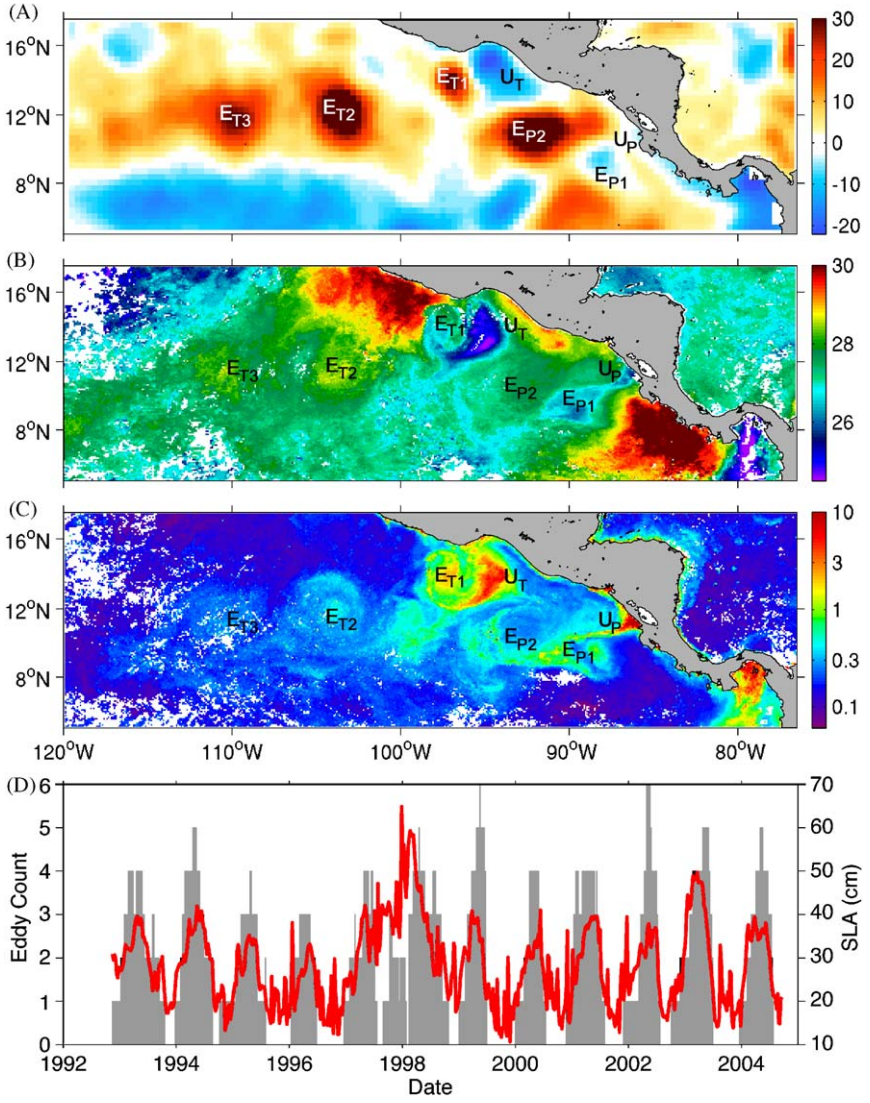

Fig. 12. Case study for the northeastern tropical Pacific region. (A) SLA (in cm) for the 7-day period 30 January–5 February 2003, (B) SST (in °C), and (C) CHL (in mg m^{-3}) for the 8-day period 2–9 February 2003. (D) Frequency histogram of number (gray) and peak intensity (red) of all eddies observed in the region between October 1992 and August 2004. SLA range in (A) is restricted for display purposes; values as high as +48 cm occur at the center of the anticyclonic eddies. Upwelling (*U*) and eddy (*E*) features associated with the Gulfs of Tehuantepec (*T*) and Papagayo (*P*) are labeled as discussed in the text.

4.3. The northeastern tropical Pacific

The dramatic effects of wintertime upwelling and eddy formation along the Central American coast are illustrated in Fig. 12. Satellite composites for early February 2003 show upwelling plumes of low SLA and SST and high CHL emanating from the Gulfs of Tehuantepec (U_T) and Papagayo (U_P). Three warm, anticyclonic eddies ($E_{T1–T3}$) are seen propagating westward, carrying high CHL water originating from the upwelling at Tehuantepec. One anticyclonic eddy (E_{P2}) with similar characteristics and one small, cold, high-CHL, cyclonic (E_{P1}) eddy are seen off the Gulf of Papagayo. Once formed at the coast, these eddies grow in diameter and propagate westward in a coherent manner at least to 120°W over the latitudinal span 8–14°N, sometimes coalescing (Palacios and Bograd, 2005).

On average, four Tehuantepec and two Papagayo eddies are formed each year. However, there is significant interannual variability in the number and intensity of these eddies, as well as in the timing and length of the eddy season (Fig. 12D; Palacios and Bograd, 2005). In particular, El Niño years are characterized by a longer eddy season, a greater number of eddies, and higher eddy intensity. This energetic system plays a major role in the transport of energy and biological constituents from the coast into the oligotrophic part of the NETP (Müller-Karger and Fuentes-Yaco, 2000; Gonzalez-Silvera et al., 2004). Also, these eddies appear to have an impact on the annual development of the nearby Costa Rica Dome (Fiedler, 2002).

4.4. The Galápagos Islands

Much of the biological richness of the waters around the Galápagos Islands is fueled by the year-round topographic upwelling of the Equatorial Undercurrent, which forms a surface plume of high phytoplankton biomass on the western side of the islands (Feldman, 1986; Palacios, 2002). While seasonal variability only has a slight effect on the extent and biomass content of the plume, as evidenced by the maps of mean CHL for February and August (Fig. 5C and D), the strongest impacts occur at the interannual and intraseasonal timescales. The Galápagos Plume Index (GPI; Fig. 13A) represents the areal extent (in km^2) of the plume as delineated by the 0.5 mg m^{-3} CHL contour in the 8-day images for the period 4 October 1997–23 December 2004 (see Section 2.6). Both the GPI and the biomass content of the plume are dominated by high-frequency variations, and with few

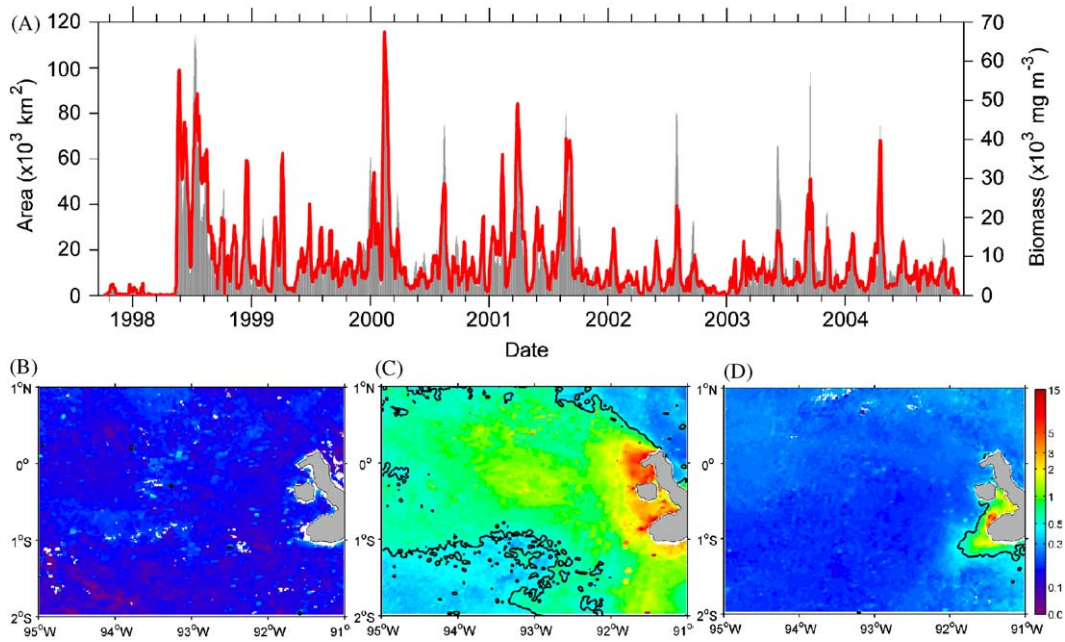

Fig. 13. Case study for the Galápagos Islands region. (A) Time series of areal extent (red) and integrated CHL biomass (gray) for the Galápagos Plume Index (GPI) for the period 4 October 1997–23 December 2004. Variations in CHL (in mg m^{-3}) plume extent for the 8-day periods centered on (B) 12 February 1998, (C) 18 February 2000, and (D) 18 February 2003.

exceptions, there is good correspondence between the two series (Fig. 13A). The GPI has a mean value of $15 \times 10^3\,km^2$ ($\pm 17 \times 10^3\,km^2$ sd) and a mean biomass of $9 \times 10^3\,mg\,m^{-3}$ ($\pm 10 \times 10^3\,mg\,m^{-3}$ sd). Both series are also punctuated by periods of limited (September 1997–May 1998; November 2002–February 2003) or enhanced (October 1999–March 2000) plume extent and magnitude, corresponding to El Niño and La Niña events, respectively (Fig. 13A). At these times, the plume may be all but absent (Fig. 13B and D), or it may grow as large as $115 \times 10^3\,km^2$ and contain upwards of $54 \times 10^3\,mg\,m^{-3}$ CHL (Fig. 13C). The Equatorial Undercurrent is known to weaken or disappear at the height of El Niño (Johnson et al., 2002), which probably leads to the suppression of the plume. On the other hand, a stronger and shallower undercurrent during La Niña (McPhaden et al., 1998) may lead to the expanded plume.

Tropical instability waves, Kelvin waves, and inertia-gravity waves are important sources of intraseasonal variability along the equator (Kessler et al., 1995, 1996; Gilbert and Mitchum, 2001) and are known to impact phytoplankton production through vertical and horizontal advective processes (Foley et al., 1997; Friedrichs and Hofmann, 2001; Gorgues et al., 2005; Waliser et al., 2005). Because the Galápagos sit within the equatorial waveguide, it is likely that the large vertical displacements of the thermocline induced by the passage of these waves persistently impact the extent and magnitude of the Galápagos Plume. A more detailed study of the forcing by equatorial waves on the Galápagos Plume is forthcoming.

5. Summary and conclusions

We have used satellite observations to describe the oceanographic characteristics of four distinct regions of the North Pacific Ocean encompassing known biological hot spots. A number of analytical techniques that can be applied to satellite data to identify and characterize hot spots in these diverse regions were employed. For each region, we have identified a variety of physical features that could potentially affect biological productivity and distributions and that can be classified by spatial scale, degree of persistence or recurrence, forcing mechanism, and biological impact:

(a) Transition zone chlorophyll front: this is a temporally persistent, seasonally migrating basin-scale frontal feature in the CNP that is known to be an important foraging and migratory corridor for apex predators.
(b) Central North Pacific eddy field: persistent and strong mesoscale features (meanders and eddies) spanning the entire CNP near 32–36°N and 28–30°N, and leading to locally enhanced (reduced) new production and predator-prey interactions in the cyclonic (anticyclonic) features.
(c) Northeastern tropical Pacific eddy field: winter wind jets crossing the Central American isthmus force the development of upwelling plumes and mesoscale eddies, which enhance productivity locally and carry coastal waters into the oligotrophic NETP.
(d) Costa Rica Dome: the persistent summer pattern of positive (cyclonic) wind stress curl lifts the thermocline, creating an offshore area of high biological production that is heavily exploited by highly migratory marine predators such as tuna, dolphins, and whales.
(e) California Current upwelling: seasonal coastal upwelling in the CCS leads to a regular cycle of high productivity on the continental shelf and a significant trophic transfer of energy at localized areas of foraging importance to top predators.
(f) California Current eddies: instabilities in the California Current lead to the formation of mesoscale eddies, which can enhance local production and transfer coastal waters and organisms offshore.
(g) Galápagos upwelling plume: a localized and highly variable plume of high phytoplankton biomass on the western side of this archipelago nevertheless leads to an important hot spot for top predators in the equatorial Pacific.

We have illustrated a variety of forcing mechanisms with timescales ranging from interannual (Rossby wave interactions in the central North Pacific) to annual (spring-summer intensification of alongshore, equatorward winds in the California Current System; wintertime wind outflow events through mountain gaps into the northeastern tropical Pacific), to intraseasonal (high-frequency equatorial waves at the Galápagos). Yet, all of these processes result in energetic mesoscale features that have marked biological signatures and relevance to top predator ecology.

In three of the regions treated in this paper (CNP, CCS, NETP), cyclonic and anticyclonic eddies are

ubiquitous features (although their forcing mechanism, size, longevity, persistence, and recurrence vary greatly between regions). It should be noted that although the sense of rotation dictates the general internal dynamics of these eddies (i.e. upwelling in cyclonic cores and downwelling in anticyclonic cores), the evolution of the local processes probably has a greater impact on biological processes. Anticyclonic eddies transition from downwelling at their center during intensification to upwelling as they decay, while the converse is true for cyclonic eddies (Flierl and McGillicuddy, 2002). In addition, the peripheries of oligotrophic anticyclonic eddies can be dynamic frontal areas of enhanced physical-biological interactions that attract top-level predators (Olson, 2002).

While satellite data offer the capacity to monitor dynamic oceanographic features and potential biological hot spots over a wide range of spatial and temporal scales, there are several severe limitations. First, only features with a significant surface signature can be observed, although subsurface fronts, eddies, and water mass features could be equally important. A number of fish species, for example, reside at depths at or below the mixed layer, and respond to physical structure at those depths (Brill and Lutcavage, 2001). Second, satellites cannot observe biological processes at the higher trophic levels or species interactions within physical features. Third, cloud cover severely limits the spatial and temporal coverage for SST and CHL. This problem is especially acute in the highly productive coastal upwelling domains of the eastern boundary currents. Finally, only some fields (e.g., SST, SLA) have sufficiently long time series of measurements to permit the description of interannual variability in the formation, location, and biological significance of dynamic oceanographic features in relation to the changing climate (Bograd et al., 2004; Polovina and Howell, 2005).

Ideally, the information most useful for the location of essential habitats of marine predators is that which comes from the animals themselves by way of satellite telemetry and an increasingly sophisticated suite of instruments carried by the animals. The emergence of organized programs (e.g., Tagging of Pacific Pelagics or TOPP; Block et al., 2002) to systematize the deployment of these tags and the analyses of the data has fundamentally changed the way essential habitat is described. Animal tracks can be mapped upon images from multiple satellite sensors that provide information on ocean structure, circulation, and production, all of which collectively define the attributes of biological hot spots. One caveat of this approach, however, is that while instrumented animals provide unique platforms to sample these features at very high resolution, not all features can be sampled by animals because the proportion of tagged animals at any given time is small relative to the population. In addition, sampling is uneven due to behavior, life history, and physiological limitations specific to each organism, as well as to tag duration. Thus, an independent satellite-based census of potential hot spots yields additional information on why particular ocean habitat is or is not utilized.

Finally, it is important to consider biological hot spots in the context of conservation and sustainable resource management. For example, if threatened or endangered species are known to utilize certain hot spots that overlap with fisheries, these features could be identified and monitored to help resource managers make decisions to mitigate adverse interactions. Furthermore, regions that encompass persistent and biologically critical oceanographic features or processes could be identified as candidate MPAs, which are traditionally defined by rigid geographical boundaries (Figs. 5A and 11A, but see Hyrenbach et al., 2000), and not necessarily constrained by the nature of the enclosed physical habitat. A more effective approach may be to use dynamic maps of biological hot spots, as obtained from remote sensing and electronic tag studies, to adaptively define regions based on immediate need. This work constitutes an early step in the process of identification and characterization of the full suite of physical features, which may eventually allow for the long-term monitoring of biological hot spots.

Acknowledgments

The authors thank the SeaWiFS Project (Code 970.2) and the GES DISC DAAC (Code 902) at the GSFC, Greenbelt, MD 20771, for the production and distribution of the ocean color data, respectively. These activities are sponsored by NASA's Mission to Planet Earth Program. We also thank Raphael M. Kudela (UCSC) for providing the 1997–2004 1-km data from MBARI's HRPT ground station. The altimeter SLA data were produced by the CLS Space Oceanography Division as part of the Environment and Climate EU ENACT project (EVK2-CT2001-00117) and with support from CNES. Paul C. Fiedler (NOAA/

NMFS/SWFSC) provided the monthly mean positions of the Costa Rica Dome used in Figs. 4 and 8. The boundary of the Galápagos Marine Reserve was kindly provided by the Unidad de Zonificación, Servicio Parque Nacional Galápagos, Ecuador. Chad King (NOAA/NOS/MBNMS) provided the boundaries for the Monterey Bay, Gulf of the Farallones, and Cordell Bank National Marine Sanctuaries used in Fig. 11. The manuscript benefited from comments by Paul C. Fiedler, Mark F. Baumgartner, and two anonymous reviewers. This work was partially supported by award No. N00014-05-1-0045 from the U.S. Office of Naval Research, National Oceanographic Partnership Program, and by the NOAA Fisheries and the Environment (FATE) program.

References

Block, B.A., Costa, D.P., Boehlert, G.W., Kochevar, R.E., 2002. Revealing pelagic habitat use: the Tagging of Pacific Pelagics program. Oceanologica Acta 25, 255–266.

Block, B.A., Teo, S.L.H., Walli, A., Boustany, A., Stokesbury, M.J.W., Farwell, C.J., Weng, K.C., Dewar, H., Williams, T.D., 2005. Electronic tagging and population structure of Atlantic bluefin tuna. Nature 434, 1121–1127.

Boersma, P.D., 1978. Breeding patterns of Galapagos penguins as an indicator of oceanographic conditions. Science 200, 1481–1483.

Boersma, P.D., Vargas, H., Merlen, G., 2005. Living laboratory in peril. Science 308, 925.

Bograd, S.J., Rabinovich, A.B., LeBlond, P.H., Shore, J.A., 1997. Observations of seamount-attached eddies in the North Pacific. Journal of Geophysical Research 102 (C6), 12441–12456.

Bograd, S.J., Foley, D.G., Schwing, F.B., Wilson, C., Laurs, R.M., Polovina, J.J., Howell, E.A., Brainard, R.E., 2004. On the seasonal and interannual migrations of the transition zone chlorophyll front. Geophysical Research Letters 31, L17204.

Brill, R.W., Lutcavage, M.E., 2001. Understanding environmental influences on movements and depth distributions of tunas and billfishes can significantly improve population assessments. American Fisheries Society Symposium 25, 179–198.

Chai, F., Jiang, M., Barber, R.T., Dugdale, R.C., Chao, Y., 2003. Interdecadal variation of the transition zone chlorophyll front, a physical-biological model simulation between 1960 and 1990. Journal of Oceanography 59, 461–475.

Chelton, D.M., Schlax, M., 1996. Global observation of oceanic Rossby waves. Science 272, 234–238.

Chelton, D.B., Freilich, M.H., Esbensen, S.K., 2000. Satellite observations of the wind jets off the Pacific coast of Central America, Part I: Case studies and statistical characteristics. Monthly Weather Review 128, 1993–2018.

Chereskin, T.K., Morris, M.Y., Niiler, P.P., Kosro, P.M., Smith, R.L., Ramp, S.R., Collins, C.A., Musgrave, D.L., 2000. Spatial and temporal characteristics of the mesoscale circulation of the California Current from eddy-resolving moored and shipboard measurements. Journal of Geophysical Research 105 (C1), 1245–1270.

Cipollini, P., Cromwell, D., Jones, M.S., Quartly, G.D., Challenor, P.G., 1997. Concurrent altimeter and infrared observations of Rossby wave propagation near 34°N in the Northeast Atlantic. Geophysical Research Letters 24, 889–892.

Cipollini, P., Cromwell, D., Challenor, P.G., Raffaglio, S., 2001. Rossby waves detected in global ocean color data. Geophysical Research Letters 28, 323–326.

Clarke, A.J., 1988. Inertial wind path and sea surface temperature patterns near the Gulf of Tehuantepec and Gulf of Papagayo. Journal of Geophysical Research 93 (C12), 15491–15501.

Coale, K.H. (Ed.), 1998. The Galápagos iron experiments: A tribute to John Martin. Deep-Sea Research II 45, 915–1150.

Croll, D.A., Tershy, B.R., Hewitt, R.P., Demer, D.A., Fiedler, P.C., Smith, S.E., Armstrong, W., Popp, J.M., Kiekhefer, T., Lopez, V.R., Urban, J., Gendron, D., 1998. An integrated approach to the foraging ecology of marine birds and mammals. Deep-Sea Research II 45, 1353–1371.

Croll, D.A., Marinovic, B., Benson, S., Chavez, F.P., Black, N., Ternullo, R., Tershy, B.R., 2005. From wind to whales: trophic links in a coastal upwelling system. Marine Ecology Progress Series 289, 117–130.

Cushing, D.H., 1990. Plankton production and year-class strength in fish populations—an update of the match-mismatch hypothesis. Advances in Marine Biology 26, 249–293.

Dorman, C.E., Winant, C.D., 1995. Buoy observations of the atmosphere along the west coast of the United States, 1981–1990. Journal of Geophysical Research 100, 16029–16044.

Ducet, N., Le Traon, P.-Y., Reverdin, G., 2000. Global high resolution mapping of ocean circulation from TOPEX/Poseidon and ERS-1/2. Journal of Geophysical Research 105, 19477–19498.

Emery, W.J., Thomson, R.E., 1997. Data Analysis Methods in Physical Oceanography. Pergamon, Exeter, UK.

Etnoyer, P., 2005. Seamount resolution in satellite-derived bathymetry. Geochemistry, Geophysics, Geosystems 6 (3), Q03004.

Feldman, G.C., 1986. Patterns of phytoplankton production around the Galápagos Islands. In: Bowman, M.J., Yentsch, C.M., Peterson, W.T. (Eds.), Tidal mixing and plankton dynamics. Lecture Notes on Coastal and Estuarine Studies 17, Springer, Berlin, pp. 77–106.

Feldman, G., Clark, D., Halpern, D., 1984. Satellite color observations of the phytoplankton distribution in the eastern equatorial Pacific during the 1982–1983 El Niño. Science 226 (4678), 1069–1071.

Fiedler, P.C., 2002. The annual cycle and biological effects of the Costa Rica Dome. Deep-Sea Research I 49, 321–338.

Fiedler, P.C., Reilly, S.B., Hewitt, R.P., Demer, D., Philbrick, V.A., Smith, S., Armstrong, W., Croll, D.A., Tershy, B.R., Mate, B.R., 1998. Blue whale habitat and prey in the California Channel Islands. Deep-Sea Research II 45, 1781–1801.

Flierl, G., McGillicuddy, D.J., 2002. Mesoscale and submesoscale physical-biological interactions. In: Robinson, A.R., et al., (Eds.), The Sea. vol. 12. Biological-Physical Interactions in The Sea. Wiley, New York, pp. 113–185.

Foley, D.G., Dickey, T.D., McPhaden, M.J., Bidigare, R.R., Lewis, M.R., Barber, R.T., Lindley, S.T., Garside, C., Manov, D.V., McNeil, J.D., 1997. Longwaves and primary productivity variations in the equatorial Pacific at 0°, 140°W. Deep-Sea Research II 44 (9–10), 1801–1826.

Friedrichs, M.A.M., Hofmann, E.E., 2001. Physical control of biological processes in the central equatorial Pacific Ocean. Deep-Sea Research I 48, 1023–1069.

Fu, L.-L., Qiu, B., 2002. Interannual variability of the North Pacific Ocean: The roles of boundary-driven and wind-driven baroclinic Rossby waves. Journal of Geophysical Research 107, 3220.

Fu, L.-L., Stammer, D., Leben, R.R., Chelton., D.B., 2003. Improved spatial resolution of ocean surface topography from the T/P-Jason-1 altimeter mission. Eos Transactions of the Amrerican Geophysical Union 84 (26), 241.

Gerber, L.R., Wooster, W.S., DeMaster, D.P., VanBlaricom, G.R., 1999. Marine mammals: New objectives in U.S. Fishery Management. Reviews in Fisheries Science 7 (1), 23–37.

Gilbert, S.A., Mitchum, G.T., 2001. Equatorial intertia-gravity waves observed in TOPEX/Poseidon sea surface heights. Geophysical Research Letters 28 (12), 2465–2468.

Glover, D.M., Wroblewski, J.S., McClain, C.R., 1994. Dynamics of the transition zone in coastal zone color scanner-sensed ocean color in the North Pacific during oceanographic spring. Journal of Geophysical Research 99, 7501–7511.

Gonzalez-Silvera, A., Santamaria-del-Angel, E., Millán-Nuñez, R., Manzo-Monroy, H., 2004. Satellite observations of mesoscale eddies in the Gulfs of Tehuantepec and Papagayo (eastern tropical Pacific). Deep-Sea Research II 51, 587–600.

Gorgues, T., Menkes, C., Aumont, O., Vialard, J., Dandonneau, Y., Bopp, L., 2005. Biogeochemical impact of tropical instability waves in the equatorial Pacific. Geophysical Research Letters 32, L24615.

Grant, P.R., 1999. Ecology and Evolution of Darwin's Finches. Princeton University Press, Princeton, New Jersey.

Gregg, W.W., Casey, N.W., McClain, C.R., 2005. Recent trends in global ocean chlorophyll. Geophysical Research Letters 32, L03606.

Hall, M.A., Donovan, G.P., 2001. Environmentalists, fishers, cetaceans and fish: is there a balance and can science help to find it? In: Evans, P.G.H., Raga, J.A. (Eds.), Marine Mammals: Biology and Conservation. Kluwer Academic/ Plenum Publishers, New York.

Hansen, D.V., Maul., G.A., 1991. Anticyclonic current rings in the eastern tropical Pacific Ocean. Journal of Geophysical Research 96 (C4), 6965–6979.

Heylings, P., Bensted-Smith, R., Altamirano, M., 2002. Zonificación e historia de la Reserva Marina de Galápagos. In: Danulat, E., Edgar, G.J. (Eds.), Reserva Marina de Galápagos, Línea Base de la Biodiversidad. Fundación Charles Darwin/Servicio Parque Nacional Galápagos, Santa Cruz, Galápagos, Ecuador, pp. 10–21.

Hickey, B.A., 1979. The California Current system: hypotheses and facts. Progress in Oceanography 8, 191–279.

Hyrenbach, K.D., Forney, K.A., Dayton, P.K., 2000. Marine protected areas and ocean basin management. Aquatic Conservation: Marine and Freshwater Ecosystems 10, 437–458.

Jacobson, L.D., Bograd, S.J., Parrish, R.H., Mendelssohn, R., Schwing, F.B., 2005. An ecosystem-based hypothesis for climatic effects on surplus production in California sardine (*Sardinops sagax*) and environmentally dependent surplus production models. Canadian Journal of Fisheries and Aquatic Sciences 62, 1782–1796.

James, M.J. (Ed.), 1991. Galápagos marine invertebrates. Taxonomy, biogeography, and evolution in Darwin's islands. Topics in Geobiology, vol. 8. Plenum Press, New York and London.

Johnson, G.C., Sloyan, B.M., Kessler, W.S., McTaggart, K.E., 2002. Direct measurements of upper ocean currents and water properties across the tropical Pacific during the 1990s. Progress in Oceanography 51 (1), 31–61.

Keiper, C.A., Ainley, D.G., Allen, S.G., Harvey, J.T., 2005. Marine mammal occurrence and ocean climate off central California, 1986 to 1994 and 1997 to 1999. Marine Ecology Progress Series 289, 285–306.

Kelly, K.A., 1988. Comment on "Empirical orthogonal function analysis of Advanced Very High Resolution Radiometer surface temperature patterns in Santa Barbara Channel" by G.S.E. Lagerloef and R.L. Bernstein. Journal of Geophysical Research 93, 15753–15754.

Kessler, W.S., McPhaden, M.J., Weickmann, K.M., 1995. Forcing of intraseasonal Kelvin waves in the equatorial Pacific. Journal of Geophysical Research 100 (C6), 10613–10631.

Kessler, W.S., Spillane, M.C., McPhaden, M.J., Harrison, D.E., 1996. Scales of variability in the equatorial Pacific inferred from the Tropical Atmosphere-Ocean buoy array. Journal of Climate 9, 2999–3024.

Kudela, R.M., Chavez, F.P., 2004. The impact of coastal runoff on ocean color during an El Niño year in Central California. Deep-Sea Research II 51, 1173–1185.

Laurs, R.M., Fiedler, P.C., Montgomery, D.C., 1984. Albacore tuna catch distributions relative to environmental features observed from satellite. Deep-Sea Research I 31, 1085–1099.

Legeckis, R., 1988. Upwelling in the Gulfs of Panama and Papagayo in the tropical Pacific during March 1985. Journal of Geophysical Research 93 (C12), 15485–15498.

Logerwell, E.A., Smith, P.E., 2001. Mesoscale eddies and survival of late stage Pacific sardine (*Sardinops sagax*) larvae. Fisheries Oceanography 10 (1), 13–25.

Lynn, R.J., Bograd, S.J., Chereskin, T.K., Huyer, A., 2003. Seasonal renewal of the California Current: The spring transition off California. Journal of Geophysical Research 108 (C8), 3279.

McGillicuddy, D., Robinson, A.R., 1997. Eddy induced nutrient supply and new production in the Sargasso Sea. Deep-Sea Research I 44, 1427–1449.

McGillicuddy, D., Robinson, A.R., Siegel, D.A., Jannasch, H.W., Johnson, R., Dickey, T.D., McNeil, J., Michaels, A.F., Knap, A.H., 1998. Influence of mesoscale eddies on new production in the Sargasso Sea. Nature 394, 263–265.

McPhaden, M.J., Busalacchi, A.J., Cheney, R., Donguy, J.-R., Gage, K.S., Halpern, D., Ji, M., Julian, P., Meyers Mitchum, G.T., Niiler, P.P., Picaut, J., Reynolds, R.W., Smith, N., Takeguchi, K., 1998. The Tropical Ocean-Global Atmosphere observing system: A decade of progress. Journal of Geophysical Research 103 (C7), 14169–14240.

Mertes, L.A.K., Warrick, J.A., 2001. Measuring flood output from 110 coastal watersheds in California with field measurements and SeaWiFS. Geology 29 (7), 659–662.

Moore, S.E., Watkins, W.A., Daher, M.A., Davies, J.R., Dahlheim, M.E., 2002. Blue whale habitat associations in

the Northwest Pacific: analysis of remotely sensed data using a Geographic Information System. Oceanography 15 (3), 20–25.

Müller-Karger, F.E., Fuentes-Yaco, C., 2000. Characteristics of wind-generated rings in the eastern tropical Pacific Ocean. Journal of Geophysical Research 105 (C1), 1271–1284.

National Marine Fisheries Service, 1999. Our Living Oceans: report on the status of U.S. living marine resources, U.S. Department of Commerce, NOAA Technical Memorandum, NMFS-F/SPO-41, 301pp.

Olson, D.B., 2002. Biophysical dynamics of ocean fronts. In: Robinson, A.R., et al. (Eds.), The Sea, Vol. 12, Biological-Physical Interactions in The Sea. Wiley, New York, pp. 187–218.

Palacios, D.M., 1999. Blue whale (*Balaenoptera musculus*) occurrence off the Galápagos Islands, 1978-1995. Journal of Cetacean Research and Management 1 (1), 41–51.

Palacios, D.M., 2002. Factors influencing the island-mass effect of the Galápagos Islands. Geophysical Research Letters 29 (23), 2134.

Palacios, D.M., 2003. Oceanographic conditions around the Galápagos Archipelago and their influence on cetacean community structure. Ph.D. Thesis, Oregon State University, Corvallis, Oregon, 178pp.

Palacios, D.M., 2004. Seasonal patterns of sea-surface temperature and ocean color around the Galápagos: regional and local influences. Deep-Sea Research II 51 (1–3), 43–57.

Palacios, D.M., Bograd, S.J., 2005. A census of Tehuantepec and Papagayo eddies in the northeastern tropical Pacific. Geophysical Research Letters 32, L23606.

Palacios, D.M., Salazar, S., 2002. Cetáceos. In: Danulat, E., Edgar, G.J. (Eds.), Reserva Marina de Galápagos, Línea Base de la Biodiversidad. Fundación Charles Darwin/Servicio Parque Nacional Galápagos, Santa Cruz, Galápagos, Ecuador, pp. 291–304.

Polito, P., Cornillon, P., 1997. Long baroclinic Rossby waves detected by TOPEX/POSEIDON. Journal of Geophysical Research 102, 3215–3235.

Polovina, J.J., Howell, E.A., 2005. Ecosystem indicators from satellite remotely sensed oceanographic data for the North Pacific. ICES Journal of Marine Science 62, 319–327.

Polovina, J.J., Kobayashi, D.R., Parker, D.M., Seki, M.P., Balazs, G.H., 2000. Turtles on the edge: Movement of loggerhead turtles (*Caretta caretta*) along oceanic fronts spanning longline fishing grounds in the central North Pacific, 1997–1998. Fisheries Oceanography 9, 1–13.

Polovina, J.J., Howell, E., Kobayashi, D.R., Seki, M.P., 2001. The transition zone chlorophyll front, a dynamic global feature defining migration and forage habitat for marine resources. Progress in Oceanography 49, 469–483.

Polovina, J.J., Balazs, G.H., Howell, E.A., Parker, D.M., Seki, M.P., Dutton, P.H., 2004. Forage and migration habitat of loggerhead (*Caretta caretta*) and olive ridley (*Lepidochelys olivacea*) sea turtles in the central North Pacific Ocean. Fisheries Oceanography 13, 36–51.

Qiu, B., 1995. Variability and energetics of the Kuroshio Extension and its recirculation gyre from the first two-year TOPEX data. Journal of Physical Oceanography 25, 1827–1842.

Reilly, S.B., Thayer, V.G., 1990. Blue whale (*Balaenoptera musculus*) distribution in the eastern tropical Pacific. Marine Mammal Science 6, 265–277.

Robinson, G., del Pino, E.M., (Eds.), 1985. El Niño in the Galápagos Islands: the 1982–83 Event. Publication of the Charles Darwin Foundation for the Galápagos Islands (Contribution No. 388), Quito, Ecuador.

Sakamoto, C.M., Karl, D.M., Jannasch, H.W., Bidigare, R.R., Letelier, R.M., Walz, P.M., Ryan, J.P., Polito, P.S., Johnson, K.S., 2004. Influence of Rossby waves on nutrient dynamics and the plankton community structure in the North Pacific subtropical gyre. Journal of Geophysical Research 109, C05032.

Salazar, S., 2002. Lobo marino y lobo peletero. In: Danulat, E., Edgar, G.J. (Eds.), Reserva Marina de Galápagos. Línea base de la biodiversidad. Fundación Charles Darwin/Servicio Parque Nacional Galápagos, Santa Cruz, Galápagos, Ecuador, pp. 267–290.

Seki, M.P., Polovina, J.J., Brainard, R.E., Bidigare, R.R., Leonard, C.L., Foley, D.G., 2001. Biological enhancement at cyclonic eddies tracked with GOES thermal imagery in Hawaiian waters. Geophysical Research Letters 28, 1583–1586.

Smith, W.H.F., Sandwell, D.T., 1997. Global seafloor topography from satellite altimetry and ship depth soundings. Science 277, 1957–1962.

Stammer, D., 1997. Global characteristics of ocean variability estimated from regional TOPEX/POSEIDON altimeter measurements. Journal of Physical Oceanography 27, 1743–1769.

Strub, P.T., Allen, J.S., Huyer, A., Smith, R.L., Beardsley, R.C., 1987. Seasonal cycle of currents, temperature, winds and sea level over the northeast Pacific continental shelf: 35–48N. Journal of Geophysical Research 92, 1507–1526.

Trasviña, A., Barton, E.D., Brown, J., Velez, H.S., Kosro, P.M., Smith, R.L., 1995. Offshore wind forcing in the Gulf of Tehuantepec, Mexico: The asymmetric circulation. Journal of Geophysical Research 100 (C10), 20649–20663.

Uz, B.M., Yoder, J.A., Osychny, V., 2001. Pumping of nutrients to ocean surface waters by the action of propagating planetary waves. Nature 409, 597–600.

Valenti, G., McClain, C., Feldman, G., Bustamante, R., 1999. SeaWiFS captures El Niño/La Niña transition. Backscatter 10 (2), 31–33.

van Woert, M.L., Price, J.M., 1993. Geosat and Advanced Very High Resolution Radiometer Observations of Oceanic and Planetary Waves Adjacent to the Hawaiian Islands. Journal of Geophysical Research 98 (C8), 14619–14650.

Waliser, D.E., Murtugudde, R., Strutton, P., Li, J.-L., 2005. Subseasonal organization of ocean chlorophyll: Prospects for prediction based on the Madden-Julian Oscillation. Geophysical Research Letters 32, L23602.

Worm, B., Lotze, H.K., Myers, R.A., 2003. Predator diversity hotspots in the blue ocean. Proceedings of the National Academy of Sciences 100 (17), 9884–9888.

Worm, B., Sandow, M., Oschlies, A., Lotze, H.K., Myers, R.A., 2005. Global patterns of predator diversity in the open oceans. Science 309, 1365–1369.

Yen, P.W., Sydeman, W.J., Hyrenbach, K.D., 2004. Marine bird and cetacean associations with bathymetric habitats and shallow-water topographies: implications for trophic transfer and conservation. Journal of Marine Systems 50, 79–99.